Journal Pre-proofs

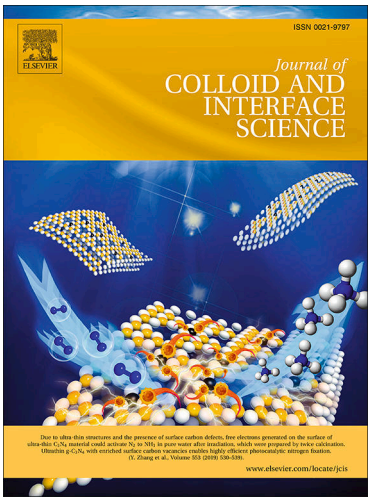

Short Communication

Elastocapillary Interactions of Thermoresponsive Microgels Across the Volume Phase Transition Temperatures

Shensheng Chen, Xin Yong

PII: S0021-9797(20)31274-1
DOI: https://doi.org/10.1016/j.jcis.2020.09.085
Reference: YJCIS 26990

To appear in: *Journal of Colloid and Interface Science*

Received Date: 24 August 2020
Revised Date: 20 September 2020
Accepted Date: 21 September 2020

Please cite this article as: S. Chen, X. Yong, Elastocapillary Interactions of Thermoresponsive Microgels Across the Volume Phase Transition Temperatures, *Journal of Colloid and Interface Science* (2020), doi: https://doi.org/10.1016/j.jcis.2020.09.085

This is a PDF file of an article that has undergone enhancements after acceptance, such as the addition of a cover page and metadata, and formatting for readability, but it is not yet the definitive version of record. This version will undergo additional copyediting, typesetting and review before it is published in its final form, but we are providing this version to give early visibility of the article. Please note that, during the production process, errors may be discovered which could affect the content, and all legal disclaimers that apply to the journal pertain.

© 2020 Elsevier Inc. All rights reserved.

Graphical Abstract

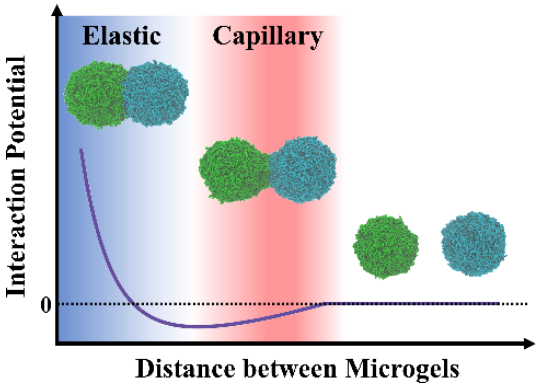

Elastocapillary Interactions of Thermoresponsive Microgels Across the Volume Phase Transition Temperatures

Shensheng Chen and Xin Yong*

Department of Mechanical Engineering, Binghamton University, Binghamton, NY 13902, USA

Emails:

Shensheng Chen: schen205@binghamton.edu

Xin Yong: xyong@binghamton.edu

Corresponding Author:

Xin Yong, PhD

Office: (+1) 607-777-4981

Fax: (+1) 607-777-4620

Journal Pre-proofs

ABSTRACT:

Hypothesis: Effective interactions of thermoresponsive microgels are known to be influenced by their volume phase transition. These soft colloids behave as repulsive spheres in the swollen state but show strong attraction in the collapsed state. We hypothesize that this transition in microgel interactions is governed by the interplay between surface tension and bulk elasticity.

*Experiment*s*:* Using dissipative particle dynamics, we modeled the interactions between two coarse-grained microgel particles having a lower critical solution temperature around 32 °C, which are suspended in an explicit solvent. The potentials of mean force between microgels with different crosslinking densities were systematically characterized in the temperature range of 12-58 °C across the volume phase transition from steer molecular dynamics simulation trajectories.

Findings: The detailed dynamics of interaction is uncovered for microgels in different states. The simulations reveal the formation of capillary bridges between collapsed microgels at high temperatures, which contributes to strong attraction at contact. An elastocapillary model based on interface thermodynamics is proposed to describe microgel interactions and accurately predicts simulation data in a wide range of temperatures and overlapping distances. The results provide important physical insights into effective interactions between soft colloids that underpin broad applications of stimuli-responsive microgels.

KEYWORDS: *microgels; volume phase transition; capillary interactions; interface thermodynamics; dissipative particle dynamics.*

1. INTRODUCTION

In a solvent, strongly repulsive particles are dispersive while attractive ones agglomerate. Weakly repulsive/attractive particles suspended in liquids can form an intermediate colloidal state without macroscopic phase separation. Effective interactions among particles determine their assembly in the solvent and thus their applications.[1] Microgels made of crosslinked networks of temperature-responsive polymers, such as poly-N-isopropylacrylamide (PNIPAM), are soft particles of sizes 10-1000 nm. These particles are able to change their shapes in aqueous solvents from a swollen state to a collapsed state across a lower or upper critical transition temperature.[2–4] The capability of tuning morphologies via temperature variations makes thermoresponsive microgel a widely used model system, not only for studying fundamental physics of colloids,[5–8]

but also for the realization of technological applications such as nanomaterials, biosensing, and drug delivery.[9,10] Understanding the effective interactions between thermoresponsive microgels is the key to theoretical modeling and practical control of the system. However, our knowledge on microgel interactions is still limited because of their highly inhomogeneous structures and temperature dependent properties.[3,11,12] An interaction potential unifying microgel phase behavior over the entire temperature range of volume phase transition remains underdeveloped.

Two simple models, the soft-sphere[4,13] and the Hertzian[14] potentials, are by far the most widely used ones to describe the interactions between two microgel particles. These soft potentials assume a microgel as an elastic repulsive sphere and relate the interaction energy u to the separation distance r between the centers of microgels as $u(r)\sim r^{-n}$ or $u(r)\sim(1-r)^n$, with the exponent n smaller than the ones used for modeling hard spheres. The soft repulsive potentials correctly describe microgel interactions in swollen states within a narrow overlapping regime.[4,15–19] Rovigatti et al. recently calculated single-particle elastic moduli of microgels across the volume phase transition and validated the Hertzian model under good solvent conditions. However, neither of the potentials captures the strong attractive behavior at high temperatures[20–22] and is able to describe the regimes where microgels significantly deform and overlap.[4,16,19,23,24] The lack of a unified expression for microgel interactions over the full temperature range and substantial overlapping states hampers our ability to theoretically model ensembles of microgels and understand their structure, thermodynamics, and dynamics. Here, we utilize a coarse-grained particle-based method to simulate PNIPAM microgel particles in explicit solvents and to investigate their effective interactions at various temperatures. By combining soft elastic repulsions of the inverse power law form and capillary contributions from the polymer-solvent interfacial energy, we propose an analytical model to predict microgel interactions across their volume phase transition in wide overlapping regimes.

2. METHODS

We characterize the interactions of thermoresponsive microgels using dissipative particle dynamics (DPD), which has been extensively used in microgel simulations[23,25–28] because of its computational efficiency and ability to capture hydrodynamics by simulating explicit solvents[29] in small-scale systems. We construct a microgel consisting of 54 000 DPD beads with 5% crosslinking density (defined by the fraction of crosslinker beads in the microgel) via an *in silico*

emulsion polymerization.[26,30,31] This approach mimics microgel synthesis in physical experiments and generates model microgels with realistic internal network structures.[32,33] The assembled microgel particle has a radius of gyration about 25 nm in the swollen state at temperature 285 K, as shown in Figure S1a. Figure S1e shows the polymer density of the microgel is not uniform in the radial direction. The profile indicates that the microgel consists of a dense core and a loose corona, which represents the structure observed in realistic ones.[3,34] We apply our previous parameter set of DPD interactions that reproduces the volume phase transition of modeled PNIPAM microgels around 32 °C with a lower critical solution temperature (LCST).[26] We simulate four representative temperatures 285 K (swollen), 308 K (transitional), 311 K (transitional), and 331 K (collapsed) that cover the entire range of volume phase transition (see Figure S1f for the variations in radius of gyration). The interaction simulations of a pair of microgel particles are performed using steered molecular dynamics (SMD). Unless stated otherwise, the simulation results are presented in DPD units. More simulation details are described in the Supporting Information.

3. RESULTS AND DISCUSSION

3.1. Morphological changes of microgels at contact

Figure 1a shows that the swollen microgels at low temperatures deform like elastic soft particles when they approach each other. During the process from contact to heavy overlapping, they squeeze each other in the impact direction while extend vertically as shown in Video S1. When temperature increases to the transitional region (see Figure 1b and Video S2), the two microgels are observed to form a small connecting gel bridge at the early stage of contact without notable bulk deformation. The bridge formation becomes more obvious and the neck grows faster in Figure 1c when temperature further increases to 331 K. The neck formation can be understood by considering microgels as viscous droplets, where the driving force of the neck growth is the Laplace pressure $\Delta p \sim \gamma R / r_{\mathrm{neck}}^2$.[35] Here, γ is the surface tension between the microgel and the solvent. R and r_{neck} are the effective radius of microgel and the neck radius, respectively. At higher temperatures, the LCST microgels will have larger γ, which then induces the neck formation and dominates the dynamics of neck growth. In this state, the behavior of microgels largely resembles that of liquid droplets except the microgels cannot coalesce at the end (see Video S3). The necking

of microgels at high temperatures indicates the surface tension must be considered in the thermoresponsive microgel interactions.

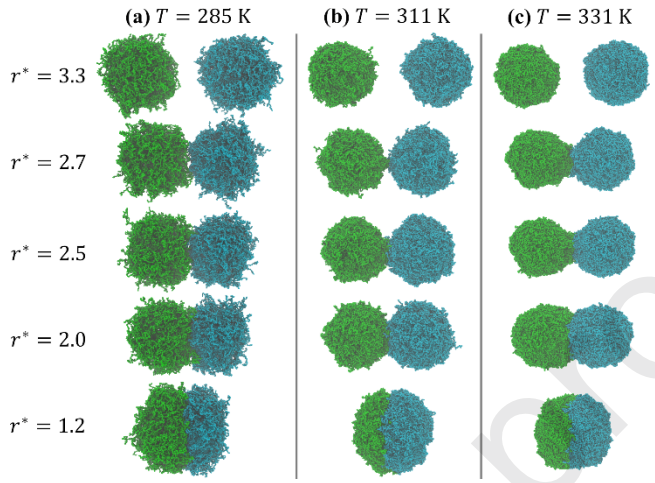

Figure 1. Simulation snapshots of two microgels being pulled towards each other in the SMD simulations at different separation distances at temperatures (a) 285 K, (b) 311 K, and (c) 331 K, which represent the swollen, transitional, and collapsed states, respectively.

3.2. Quantification of pair interactions

The effective interaction potentials are quantified in the form of the potential of mean force profiles extracted from SMD. To reduce nonequilibrium effects,[36,37] a strong spring with a force constant of 5000 (corresponding to 1.24×104 kJ·mol^{-1}·nm^{-2}) [38,39] is introduced to connect the centers of mass (COM) of two microgels and pulls them toward each other at a speed v of 0.0024 (corresponding to 0.025 Å/ns) until the normalized inter-distance $r^* = r(t)/R_g(T)$ reduces to 1.1, at which the two microgels significantly overlap.[16] Here, $r(t)$ is the instantaneous distance between the microgel COM and $R_g(T)$ is the radius of gyration of the equilibrium microgel at the corresponding temperature. The Jarzynski's equality relates the accumulated work W done by the pulling spring in SMD to the free energy difference ΔG or potential mean force (PMF) by PMF $= -\frac{1}{\beta}\ln\langle\exp(-\beta W)\rangle$, with $\beta = 1/k_B T$ being the inverse of thermal energy.[40,41] The ensemble average $\langle\cdots\rangle$ is usually estimated by the second order expansion using a limited number of SMD

simulation trajectories, which yields $\mathrm{PMF} = \langle W \rangle - \frac{\beta}{2}[\langle W^2 \rangle - \langle W \rangle^2]$.[37] In the present work, we calculate the PMF based on the accumulated work (Figure S2a) from 10 SMD trajectories for each temperature at a given crosslinking density. We note that biased and steered dynamics algorithms need to be implemented cautiously to prevent the onset of unphysical behavior in nonequilibrium simulations.[42] We conducted benchmark simulations with multiple pulling velocities and confirmed sufficient relaxation of polymer network under deformation at $v = 0.025$ Å/ns. The corresponding Peclet numbers $\mathrm{Pe} = vR_g/D$ defined using the collective diffusivity of polymer network[43] are on the order of 10^{-2}, which also indicates nonequilibrium effects are minimized given the available computational resource. Figure 2 shows the PMF of a pair of microgel particles along the pulling coordinate is clearly temperature dependent. Increasing temperature results in gradual weakening of repulsion between microgels at contact and eventually changes the interaction to effective attraction in the weakly overlapping regime, as shown in the negative portion of PMF profiles. This repulsion to attraction transition qualitatively agrees with the nature of PNIPAM microgels.[44] Below, we propose an analytical model based on interfacial thermodynamics to describe the effective potentials that cover the entire temperature range from the swollen to collapsed states.

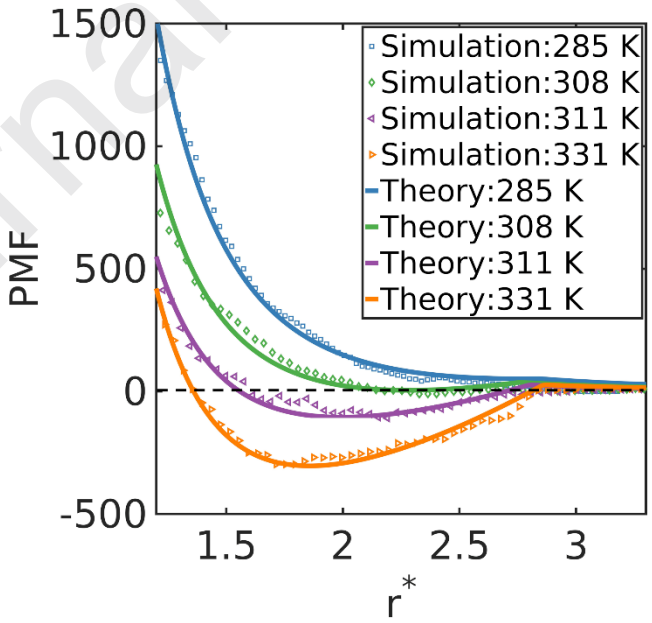

Journal Pre-proofs

Figure 2. PMF profiles for two microgels with 5% crosslink densities interacting at temperatures 285 K, 308 K, 311 K, and 331K. Solid lines are the effective interaction potentials predicted by the proposed elastocapillary model. The black dashed line marks the zero-potential level that separates attraction and repulsion regions.

3.3. Elastocapillarity in microgel interactions

The soft-sphere potential has been widely used to describe microgel interactions.[4] It takes the form as $u(r) = \varepsilon(\sigma/r)^n$, where r is the separation between the centers of the particles, σ is the characteristic microgel size, and ε is the interaction strength. The expression mainly considers the elastic repulsion when microgels overlap and does not include any attractive contributions. We hypothesize that the temperature effect on the interactions of thermoresponsive microgels can be quantitatively described through considering the temperature dependence of surface free energy in the system. The surface free energy of the two microgels at a distance r can be given as $f_s = A(r)\gamma$, where $A(r)$ is the total surface area of microgels at distance r. Taking two separated microgels as the reference state, the reduction of microgel surfaces exposed to water upon overlapping causes the change in surface energy $\Delta f_s = \Delta A(r)\gamma$. The total area reduction can be estimated by $\Delta A(r) = \Delta A_1(r) + \Delta A_2(r)$, where ΔA_1 is the surface area loss due to overlapping and ΔA_2 is the surface area gain of inflated microgels subject to conservation of volume. The surface area change is schematically shown in Figure 3. Because the changes of area and volume are interdependent, accurate determination of $\Delta A(r)$ requires ΔA_1 and ΔA_2 to be self-consistent and accounts for the deformation of microgels. Here, we simplify the calculation by assuming that microgels preserve a spherical shape, as well as ignoring self-consistency between ΔA_1 and ΔA_2. For microgels with an effective radius of R, we can estimate $\Delta A_1 \approx 4\pi R(R - r/2)$ and $A_2(r) \approx 8\pi \left[R^3 + (R - r/2)^2(2R + r/2)/4\right]^{2/3} - 8\pi R^2$. The effective radius is estimated as half of the distance at which microgels start to interact, based on the PMF profiles. Notably, this expression of $\Delta A(r)$ becomes less accurate as the separation distance r decreases. Surface tension is given by the Flory-Huggins parameters for the polymer-solvent interaction $\chi(T)$ as $\gamma = [\chi(T)/6]^{0.5}\rho k_B T$, where ρ is polymer number density.[45,46] In general, χ increases with temperature for PNIPAM

microgels. In this work, we use an expression of $\chi(T)$ validated in previous DPD simulations of PNIPAM microgels[26] with details given in the Supporting Information.

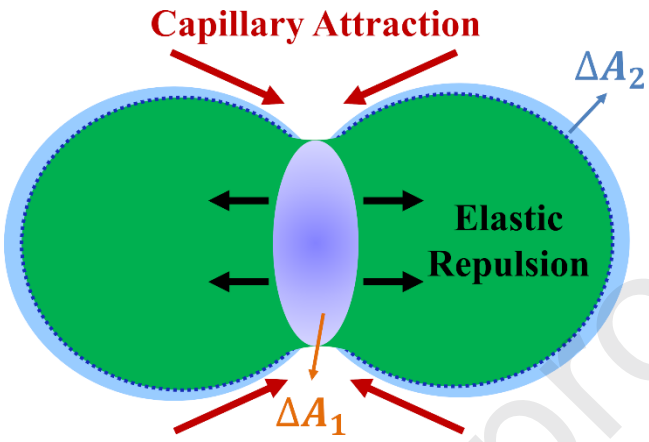

Figure 3. Schematic diagram of microgel interactions governed by the competition between surface tension and elasticity.

Taking the surface free energy into account, we propose a theoretical model of microgel interactions that couples soft elastic repulsion and temperature-dependent capillary attraction (Figure 3). The formula is given as $U(r,T) = \varepsilon(\sigma/r)^n + \Delta f_s(r,T)$. We select the characteristic microgel size σ as the radius of gyration R_g at the corresponding temperature with n and ε being the fitting parameters. Figure 2(b) shows the model agrees well with our simulation results across all investigated temperatures while covering wide overlapping regimes (from no contact to $r^* = 1.2$). The best fit of the power coefficient shows $n = 4.0$, 4.1, 4.2, and 4.4 for temperatures of 285 K, 308 K, 311 K, and 331 K, respectively. The attractive component of the interaction potential at high temperatures can be well explained by this elastocapillary model. At low temperatures, the Flory-Huggins parameter between microgel and water is small. The limited reduction in surface free energy is offset by the significant elastic energy increase from the microgel deformation. This is consistent with the successes of previous soft-repulsive models in explaining microgel interactions at low temperatures. As microgels undergo the volume phase transition into the collapsed state, the surface energy becomes dominant at contact, which is manifested in the effective attraction region shown in the PMF profiles. Because microgels have been shown to have

a core-corona structure, the elastic contribution upon overlapping does not scale linearly. The outer corona region can be approximately treated as polymer brushes, in which the elastic repulsion is not divergent upon overlapping.[47] The surface tension induced attraction dominates at early times, as the dilute polymers in the corona region can only provide weak repulsion.

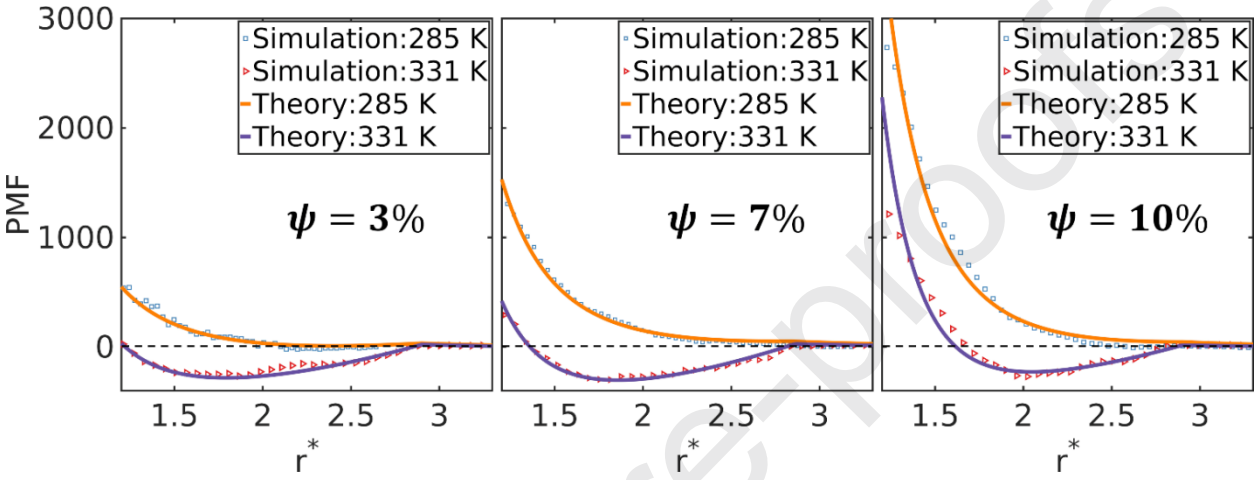

Figure 4. PMF profiles of interacting microgels at low (285 K) and high (331 K) temperatures for crosslinker densities at 3%, 7%, and 10%, respectively. The dashed lines denote the zero-potential position.

We further test the model for microgels with different crosslinking densities ψ and probe the effect of microgel structure on the interaction potential. The influence of crosslink densities on the microgel size is quantified in Figure S1f in the swollen and collapsed states. Figure 4 plots the PMF profiles of microgels for crosslinking number densities at 3%, 7%, and 10% at the two representative temperatures of 285 K and 331 K (corresponding accumulated work profiles are plotted in Figures S2b and S2c). Increasing the crosslinking density of the microgels results in stronger repulsion in both swollen and collapsed states. The attractive potential well becomes shallower and narrower when crosslinking density increases, which is attributed to increased elastic moduli and stronger repulsion of highly crosslinked microgels.[18,48] Figure 4 also demonstrates good agreement between the analytical model and simulation results for all tested crosslinking densities at the two distinct temperatures. The difference in crosslinking density is

reflected in the interaction strength ε and exponent n of the elastic repulsion term. The best fit of the simulation data to the analytical model shows increasing values of n as crosslinking densities increases (the complete values of n and ε are listed in Table S1). The increase in the power-law exponent indicates enhanced mechanical properties of microgel particles. The more obvious surface tension effect in weakly crosslinked microgels demonstrates its fluidic characteristics.

3.4. Discussion of the theoretical model

The combination of soft-sphere repulsion and surface-tension induced attraction in our model is proposed in the light of adhesive elastic contact models in contact mechanics.[49,50] The Johnson–Kendall–Roberts (JKR) theory[51] describes the deformation of two elastic objects at contact is governed by the interplay between solid-solid adhesion energy and elasticity. The use of the simple adhesion energy has been validated for particle size larger than a threshold value around 10 μm. For colloidal particles suspended in a solvent with a characteristic particle length smaller than the threshold value, solid-fluid surface tension will dominate the contact process, as the surface energy scale is much larger than the elasticity energy scale in small deformations.[52] Microgel particles typically have sizes of 10-1000 nm,[3,4] thus it is necessary to explicitly include surface tension in their interactions. However, microgels behave more complex than elastic solid particles as they possess heterogeneous structures of mixed polymers and solvent with low solid content. To capture the fluidic nature of microgels, the capillary contribution in our model is derived according to interfacial thermodynamics, which considers polymer-solvent surface tension as in droplet coalescence instead of solid-solid adhesion in contact mechanics. The soft sphere repulsion follows a solid mechanics approach, which represents the structural integrity of microgels. Thus, the analytical model proposed in this work can be viewed as a hybrid model that captures the semi-solid/semi-liquid nature of microgels.

Compared to the repulsive sphere models, the new model highlights the attractive regime of the collapsed microgels. The attractive regime will contribute significantly to macroscopic properties of microgels, in particular rheology[53–55] and nano-/micro-fabrication.[56] For example, the rheological properties of microgel suspensions are critical to 3D printing applications.[57] Strongly attractive microgels have the potential to form colloidal gel structures[58,59] other than well-documented crystalline arrays.[60] A clear understanding of pair interactions of thermoresponsive

microgels in changing environmental conditions lays the groundwork for large-scale applications based on microgel jamming, assembly, and pattern formation.

4. CONCLUSIONS

The effective interaction between thermoresponsive microgels is an important question in the field of soft matter which remains understudied.[23,24] Only a few studies were focused directly on the effective interactions between microgels[16–19] and the analysis was mostly limited to the swollen state (i.e., low temperature regimes for LCST microgels). An analytical expression for the interparticle potential which covers the entire temperature range of microgel swelling-deswelling transition has yet to be developed. Previous experiments showed that the effective interactions between microgels change from repulsive to attractive when temperature increases (i.e., microgels change from the swollen state to the collapsed states).[20–22,53] In this study, we hypothesize that the transition in the effective interaction is determined by the temperature-dependent surface tension between the polymer and solvent. We exploit dissipative particle dynamics to test this hypothesis. At low temperatures, the swollen microgels are shown to be repulsive and qualitatively agrees with the widely used soft repulsive models. However, we observe that two microgels strongly attract to each other at high temperatures, which is consistent with experimental results.[20,21,44] The simulations also provide insights into the detailed dynamics of interaction, which is challenging to probe in experiments. We discover an intriguing behavior of capillary bridge formation between collapsed microgels at contact. The results suggest the existing soft-repulsive potential models have major limitations in the attraction dominant regime.

We propose a theoretical model of effective interactions across the volume phase transition temperature and in a wide overlapping distance range, which describes the balance of surface energy loss and elastic strain energy gain. The good agreement between the theoretical predictions and simulation data confirms that the effective attraction is driven by surface tension, which dominates elasticity at high temperatures. In addition, we validate the model for microgels with different network structures by turning their crosslinking densities. Recent experiments and simulations have shown the effective interactions between thermoresponsive microgels is dependent on temperature and structure.[18,19] By explicitly incorporating the temperature dependent of surface energy, our model reveals the detailed mechanism that relates temperature and structure to the effective interaction. Our finding also suggests that the solvent effect must be considered

when dealing with microgel interactions. The dynamic behavior reported here highlights fundamental differences between microgel particles and conventional hard-sphere-like colloids.

While this work is focused on fundamental interaction mechanism between two identical neutral microgels, it would be of interest to explore more complex microgel systems in future studies, such as specifically structuralized microgels and ionic microgels.[61,62] Systematic investigations are also needed to exploit the relationship between pair interactions and large-scale microgel assembly. Moreover, the capillary bridge formation and necking dynamics at high temperatures reported in this work highlight the fluidic characteristic of microgel particles. It is important to fully understand the fundamental differences among liquid droplets, collapsed microgels, and hard-sphere particles in future work.

ACKNOWLEDGMENTS

X.Y. gratefully acknowledges funding from the National Science Foundation under Grant No. CMMI-1939362 for partial support of S.C. Generous allocation of computing time was provided by the Center for Functional Nanomaterials, which is a U.S. DOE Office of Science Facility, at Brookhaven National Laboratory under Contract No. DESC0012704.

REFERENCES

(1) Saunders, B. R.; Vincent, B. Microgel Particles as Model Colloids: Theory, Properties and Applications. *Adv. Colloid Interface Sci.* **1999**, *80*, 1–25.

(2) Senff, H.; Richtering, W. Temperature Sensitive Microgel Suspensions: Colloidal Phase Behavior and Rheology of Soft Spheres. *J. Chem. Phys.* **1999**, *111*, 1705–1711.

(3) Plamper, F. A.; Richtering, W. Functional Microgels and Microgel Systems. *Acc. Chem. Res.* **2017**, *50*, 131–140.

(4) Heyes, D. M.; Brańka, A. C. Interactions between Microgel Particles. *Soft Matter* **2009**, *5*, 2681.

(5) Mohanty, P. S.; Bagheri, P.; Nöjd, S.; Yethiraj, A.; Schurtenberger, P. Multiple Path-Dependent Routes for Phase-Transition Kinetics in Thermoresponsive and Field-Responsive Ultrasoft Colloids. *Phys. Rev. X* **2015**, *5*, 011030.

(6) Peng, Y.; Wang, Z.; Alsayed, A. M.; Yodh, A. G.; Han, Y. Melting of Colloidal Crystal Films. *Phys. Rev. Lett.* **2010**, *104*, 205703.

(7) Zhang, Z.; Xu, N.; Chen, D. T. N.; Yunker, P.; Alsayed, A. M.; Aptowicz, K. B.; Habdas, P.; Liu, A. J.; Nagel, S. R.; Yodh, A. G. Thermal Vestige of the Zero-Temperature Jamming Transition. *Nature* **2009**, *459*, 230–233.

(8) Hilhorst, J.; Petukhov, A. V. Variable Dislocation Widths in Colloidal Crystals of Soft Thermosensitive Spheres. *Phys. Rev. Lett.* **2011**, *107*, 095501.

(9) Fernández-Barbero, A.; Suárez, I. J.; Sierra-Martín, B.; Fernández-Nieves, A.; de las Nieves, F. J.; Marquez, M.; Rubio-Retama, J.; López-Cabarcos, E. Gels and Microgels for Nanotechnological Applications. *Adv. Colloid Interface Sci.* **2009**, *147–148*, 88–108.

(10) Hamidi, M.; Azadi, A.; Rafiei, P. Hydrogel Nanoparticles in Drug Delivery. *Adv. Drug Deliv. Rev.* **2008**, *60*, 1638–1649.

(11) Keidel, R.; Ghavami, A.; Lugo, D. M.; Lotze, G.; Virtanen, O.; Beumers, P.; Pedersen, J. S.; Bardow, A.; Winkler, R. G.; Richtering, W. Time-Resolved Structural Evolution during the Collapse of Responsive Hydrogels: The Microgel-to-Particle Transition. *Sci. Adv.* **2018**, *4*, eaao7086.

(12) Holmqvist, P.; Mohanty, P. S.; Nägele, G.; Schurtenberger, P.; Heinen, M. Structure and Dynamics of Loosely Cross-Linked Ionic Microgel Dispersions in the Fluid Regime. *Phys. Rev. Lett.* **2012**, *109*, 048302.

(13) Israelachvili, J. N. *Intermolecular and Surface Forces*; Third.; Academic Press, Inc., **2011**.

(14) Pàmies, J. C.; Cacciuto, A.; Frenkel, D. Phase Diagram of Hertzian Spheres. *J. Chem. Phys.* **2009**, *131*, 044514.

(15) Pyett, S.; Richtering, W. Structures and Dynamics of Thermosensitive Microgel Suspensions Studied with Three-Dimensional Cross-Correlated Light Scattering. *J. Chem. Phys.* **2005**, *122*, 034709.

Journal Pre-proofs

(16) Ahualli, S.; Martín-Molina, A.; Maroto-Centeno, J. A.; Quesada-Pérez, M. Interaction between Ideal Neutral Nanogels: A Monte Carlo Simulation Study. *Macromolecules* **2017**, *50*, 2229–2238.

(17) Mohanty, P. S.; Paloli, D.; Crassous, J. J.; Zaccarelli, E.; Schurtenberger, P. Effective Interactions between Soft-Repulsive Colloids: Experiments, Theory, and Simulations. *J. Chem. Phys.* **2014**, *140*, 094901.

(18) Rovigatti, L.; Gnan, N.; Ninarello, A.; Zaccarelli, E. Connecting Elasticity and Effective Interactions of Neutral Microgels: The Validity of the Hertzian Model. *Macromolecules* **2019**, *52*, 4895–4906.

(19) Bergman, M. J.; Gnan, N.; Obiols-Rabasa, M.; Meijer, J.-M.; Rovigatti, L.; Zaccarelli, E.; Schurtenberger, P. A New Look at Effective Interactions between Microgel Particles. *Nat. Commun.* **2018**, *9*, 5039.

(20) Wu, J.; Huang, G.; Hu, Z. Interparticle Potential and the Phase Behavior of Temperature-Sensitive Microgel Dispersions. *Macromolecules* **2003**, *36*, 440–448.

(21) Romeo, G.; Fernandez-Nieves, A.; Wyss, H. M.; Acierno, D.; Weitz, D. A. Temperature-Controlled Transitions Between Glass, Liquid, and Gel States in Dense p-NIPA Suspensions. *Adv. Mater.* **2010**, *22*, 3441–3445.

(22) Stieger, M.; Pedersen, J. S.; Lindner, P.; Richtering, W. Are Thermoresponsive Microgels Model Systems for Concentrated Colloidal Suspensions? A Rheology and Small-Angle Neutron Scattering Study. *Langmuir* **2004**, *20*, 7283–7292.

(23) Martín-Molina, A.; Quesada-Pérez, M. A Review of Coarse-Grained Simulations of Nanogel and Microgel Particles. *J. Mol. Liq.* **2019**, *280*, 374–381.

(24) Brijitta, J.; Schurtenberger, P. Responsive Hydrogel Colloids: Structure, Interactions, Phase Behavior, and Equilibrium and Nonequilibrium Transitions of Microgel Dispersions. *Curr. Opin. Colloid Interface Sci.* **2019**, *40*, 87–103.

(25) Hoppe Alvarez, L.; Eisold, S.; Gumerov, R. A.; Strauch, M.; Rudov, A. A.; Lenssen, P.; Merhof, D.; Potemkin, I. I.; Simon, U.; Wöll, D. Deformation of Microgels at Solid–Liquid Interfaces Visualized in Three-Dimension. *Nano Lett.* **2019**, *19*, 8862–8867.

(26) Yong, X.; Kuksenok, O.; Matyjaszewski, K.; Balazs, A. C. Harnessing Interfacially-Active Nanorods to Regenerate Severed Polymer Gels. *Nano Lett.* **2013**, *13*, 6269–6274.

(27) Chen, S.; Yong, X. Dissipative Particle Dynamics Modeling of Hydrogel Swelling by Osmotic Ensemble Method. *J. Chem. Phys.* **2018**, *149*, 094904.

(28) Camerin, F.; Gnan, N.; Rovigatti, L.; Zaccarelli, E. Modelling Realistic Microgels in an Explicit Solvent. *Sci. Rep.* **2018**, *8*, 14426.

(29) Groot, R. D.; Warren, P. B. Dissipative Particle Dynamics: Bridging the Gap between Atomistic and Mesoscopic Simulation. *J. Chem. Phys.* **1997**, *107*, 4423–4435.

(30) Gnan, N.; Rovigatti, L.; Bergman, M.; Zaccarelli, E. In Silico Synthesis of Microgel Particles. *Macromolecules* **2017**, *50*, 8777–8786.

(31) Yong, X.; Kuksenok, O.; Balazs, A. C. Modeling Free Radical Polymerization Using Dissipative Particle Dynamics. *Polymer (Guildf).* **2015**.

(32) Tobita, H.; Kumagai, M.; Aoyagi, N. Microgel Formation in Emulsion Polymerization. *Polymer (Guildf).* **2000**, *41*, 481–487.

(33) Butté, A.; Storti, G.; Morbidelli, M. Microgel Formation in Emulsion Polymerization. *Macromol. Theory Simulations* **2007**, *16*, 441–457.

(34) Stieger, M.; Richtering, W.; Pedersen, J. S.; Lindner, P. Small-Angle Neutron Scattering Study of Structural Changes in Temperature Sensitive Microgel Colloids. *J. Chem. Phys.* **2004**, *120*, 6197–6206.

(35) Paulsen, J. D.; Carmigniani, R.; Kannan, A.; Burton, J. C.; Nagel, S. R. Coalescence of Bubbles and Drops in an Outer Fluid. *Nat. Commun.* **2014**, *5*, 3182.

(36) Yu, T.; Lee, O.-S.; Schatz, G. C. Steered Molecular Dynamics Studies of the Potential of Mean Force for Peptide Amphiphile Self-Assembly into Cylindrical Nanofibers. *J. Phys. Chem. A* **2013**, *117*, 7453–7460.

(37) Park, S.; Schulten, K. Calculating Potentials of Mean Force from Steered Molecular Dynamics Simulations. *J. Chem. Phys.* **2004**, *120*, 5946–5961.

Journal Pre-proofs

(38) Fan, H.; Striolo, A. Mechanistic Study of Droplets Coalescence in Pickering Emulsions. *Soft Matter*, **2012**, *8*, 9533.

(39) Qin, S.; Yong, X. Controlling the Stability of Pickering Emulsions by PH-Responsive Nanoparticles. *Soft Matter* **2019**, *15*, 3291–3300.

(40) Jarzynski, C. Nonequilibrium Equality for Free Energy Differences. *Phys. Rev. Lett.* **1997**, *78*, 2690–2693.

(41) Jarzynski, C. Equilibrium Free-Energy Differences from Nonequilibrium Measurements: A Master-Equation Approach. *Phys. Rev. E* **1997**, *56*, 5018–5035.

(42) Sicard, F.; Striolo, A. Numerical Analysis of Pickering Emulsion Stability: Insights from ABMD Simulations. *Faraday Discuss.* **2016**, *191*, 287–304.

(43) Tanaka, T.; Fillmore, D. J. Kinetics of Swelling of Gels. *J. Chem. Phys.* **1979**, *70*, 1214–1218.

(44) Wu, J.; Zhou, B.; Hu, Z. Phase Behavior of Thermally Responsive Microgel Colloids. *Phys. Rev. Lett.* **2003**, *90*, 048304.

(45) Tang, T.-Y.; Zhou, Y.; Arya, G. Interfacial Assembly of Tunable Anisotropic Nanoparticle Architectures. *ACS Nano* **2019**, *13*, 4111–4123.

(46) Helfand, E.; Tagami, Y. Theory of the Interface Between Immiscible Polymers. *J. Chem. Phys.* **1972**, *57*, 1812–1813.

(47) Scheffold, F.; Díaz-Leyva, P.; Reufer, M.; Ben Braham, N.; Lynch, I.; Harden, J. L. Brushlike Interactions between Thermoresponsive Microgel Particles. *Phys. Rev. Lett.* **2010**, *104*, 128304.

(48) Senff, H.; Richtering, W. Influence of Cross-Link Density on Rheological Properties of Temperature-Sensitive Microgel Suspensions. *Colloid Polym. Sci.* **2000**, *278*, 830–840.

(49) Ghaednia, H.; Wang, X.; Saha, S.; Xu, Y.; Sharma, A.; Jackson, R. L. A Review of Elastic–Plastic Contact Mechanics. *Appl. Mech. Rev.* **2017**, *69*.

(50) Shull, K. R. Contact Mechanics and the Adhesion of Soft Solids. *Mater. Sci. Eng. R Reports* **2002**, *36*, 1–45.

Journal Pre-proofs

(51) Johnson, K., Kendall, K. & Roberts, A. Surface Energy and the Contact of Elastic Solids. *Proc. R. Soc. London. A. Math. Phys. Sci.* **1971**, *324*, 301–313.

(52) Style, R. W.; Hyland, C.; Boltyanskiy, R.; Wettlaufer, J. S.; Dufresne, E. R. Surface Tension and Contact with Soft Elastic Solids. *Nat. Commun.* **2013**, *4*, 2728.

(53) Shao, Z.; Negi, A. S.; Osuji, C. O. Role of Interparticle Attraction in the Yielding Response of Microgel Suspensions. *Soft Matter* **2013**, *9*, 5492.

(54) Minami, S.; Watanabe, T.; Suzuki, D.; Urayama, K. Viscoelasticity of Dense Suspensions of Thermosensitive Microgel Mixtures Undergoing Colloidal Gelation. *Soft Matter* **2018**, *14*, 1596–1607.

(55) Koumakis, N.; Petekidis, G. Two Step Yielding in Attractive Colloids: Transition from Gels to Attractive Glasses. *Soft Matter* **2011**, *7*, 2456.

(56) Lyon, L. A.; Meng, Z.; Singh, N.; Sorrell, C. D.; St. John, A. Thermoresponsive Microgel-Based Materials. *Chem. Soc. Rev.* **2009**, *38*, 865.

(57) Highley, C. B.; Song, K. H.; Daly, A. C.; Burdick, J. A. Jammed Microgel Inks for 3D Printing Applications. *Adv. Sci.* **2019**, *6*, 1801076.

(58) Immink, J. N.; Maris, J. J. E.; Crassous, J. J.; Stenhammar, J.; Schurtenberger, P. Reversible Formation of Thermoresponsive Binary Particle Gels with Tunable Structural and Mechanical Properties. *ACS Nano* **2019**, *13*, 3292–3300.

(59) Appel, J.; Fölker, B.; Sprakel, J. Mechanics at the Glass-to-Gel Transition of Thermoresponsive Microgel Suspensions. *Soft Matter* **2016**, *12*, 2515–2522.

(60) Geisel, K.; Richtering, W.; Isa, L. Highly Ordered 2D Microgel Arrays: Compression versus Self-Assembly. *Soft Matter* **2014**, *10*, 7968–7976.

(61) Berndt, I.; Pedersen, J. S.; Richtering, W. Temperature-Sensitive Core–Shell Microgel Particles with Dense Shell. *Angew. Chemie* **2006**, *118*, 1769–1773.

(62) Gottwald, D.; Likos, C. N.; Kahl, G.; Löwen, H. Ionic Microgels as Model Systems for Colloids with an Ultrasoft Electrosteric Repulsion: Structure and Thermodynamics. *J. Chem. Phys.* **2005**, *122*, 074903.

Journal Pre-proofs

Supplemental Material for

Elastocapillary Interactions of Thermoresponsive Microgels Across the Volume Phase Transition Temperatures

Shensheng Chen and Xin Yong*
Department of Mechanical Engineering, Binghamton University, Binghamton, NY 13902, USA
* xyong@binghamton.edu

A. Dissipative particle dynamics

Dissipative particle dynamics (DPD)[1] simulations are used to study the effective interaction in microgel systems. In DPD, all solvent beads and polymer segments are explicitly included and represented as beads of equal mass *m*, where each bead represents a group of molecules. The dynamics of these beads are governed by pairwise potentials between interacting beads according to Newton's second law $m\left(d\mathbf{v}_i / dt\right) = -\nabla U\left(\mathbf{r}_i\right)$. The resulting force acted on beads i contains three terms including conservative force, dissipative force, and random force: $\mathbf{F}_i = \sum\left(\mathbf{F}_{ij}^{\mathrm{C}} + \mathbf{F}_{ij}^{\mathrm{D}} + \mathbf{F}_{ij}^{\mathrm{R}}\right)$. The sum is carried out for all beads *j* within a certain cutoff radius r_{c} from bead i. The conservative part is given by $\mathbf{F}_{ij}^{\mathrm{C}} = a_{ij}(1 - r_{ij} / r_{\mathrm{c}})\mathbf{e}_{ij}$, where a_{ij} is the maximum repulsion between beads i and j; $r_{ij} = \left|\mathbf{r}_i - \mathbf{r}_j\right| / r_{\mathrm{c}}$ is the inter-bead distance; and $\mathbf{e}_{ij} = \left(\mathbf{r}_i - \mathbf{r}_j\right) / \left|\mathbf{r}_i - \mathbf{r}_j\right|$ represents the force direction. It is convenient to pick the cutoff r_{c} as the characteristic length of the DPD simulation. The interaction strength between the beads representing the same species is set to 25 to reproduce the compressibility of water.[1] The miscibility between microgel polymer beads and water beads is controlled by the repulsion coefficient a_{ij}, which is dependent on temperature for thermoresponsive polymers and will be discussed later. Compared with the Lennard-Jones potential used in molecular dynamics, the capped linear repulsion permits the use of much larger time steps in DPD and allows simulations

Journal Pre-proofs

on larger time scales. The dissipative force $\mathbf{F}_{ij}^{\mathrm{D}}$ is proportional to the relative velocity of two beads $\mathbf{v}_{ij} = \mathbf{v}_i - \mathbf{v}_j$, given by $\mathbf{F}_{ij}^{\mathrm{D}} = -\alpha w_{\mathrm{D}}(r_{ij})(\mathbf{e}_{ij} \cdot \mathbf{v}_{ij})\mathbf{e}_{ij}$. The random force $\mathbf{F}_{ij}^{\mathrm{R}} = \beta w_{\mathrm{R}}(r_{ij})\xi_{ij}\mathbf{e}_{ij}$ represents a Gaussian white noise, where ξ_{ij} is a random variable satisfying $\langle \xi_{ij}(t) \rangle = 0$ and $\langle \xi_{ij}(t)\xi_{i'j'}(t') \rangle = (\delta_{ii'}\delta_{jj'} + \delta_{ij'}\delta_{ji'})\delta(t-t')$. w_{D} and w_{R} are arbitrary weight functions dependent on the interparticle distance. The two parameters α and β determine the strength of viscous dissipation and the noise amplitude, respectively. The temperature of a DPD system T is controlled inherently through the fluctuation-dissipation theorem, which demands $\left[w_{\mathrm{R}}\left(r_{ij}\right) \right]^2 = w_{\mathrm{D}}\left(r_{ij}\right) = \left(1 - r_{ij}/r_{\mathrm{c}}\right)^2$ and $\beta^2 = 2k_{\mathrm{B}}T\alpha$, with k_{B} being the Boltzmann constant. The energy of thermal fluctuation $k_{\mathrm{B}}T$ is often chosen as the characteristic energy. Because our simulation involves temperature variations, we select room temperature $T_0 = 298.15$ K as the reference temperature and $k_{\mathrm{B}}T_0$ as the reference energy scale. The reduced temperature is therefore defined as $T^* = T/T_0$. Based on the dimensional analysis, the characteristic time for DPD is thus given as $\tau = \sqrt{mr_{\mathrm{c}}^2 / k_{\mathrm{B}}T_0}$. According to the convention of DPD, we present the simulation results in reduced units with r_{c}, m, and $k_{\mathrm{B}}T$ all set to one, which also give $\tau = 1$. The remaining simulation parameters are $\alpha = 4.5$, simulation time step $\Delta t = 0.02$, and total number density $\rho_0 = 3$. For SMD simulations, two microgels are initially equilibrium in a simulation domain of $130 \times 70 \times 70$ with a fix center to center distance at 60 at a target temperature.

B. *In silico* synthesis of microgel particles

We perform simulated emulsion polymerization to construct microgels with realistic internal structures. We apply our previously developed atom transfer radical polymerization

Journal Pre-proofs

(ATRP) scheme in the DPD framework to simulate the controlled/living copolymerization of monomer and crosslinker to from a microgel.[2] Monomers, crosslinkers with a number concentration ψ, and 50% of water beads are first placed in a spherical domain of radius 20 in the center of a cubic simulation box with the dimensions of $50\times50\times50$. The outside of the spherical domain is filled with a second solvent immiscible with water so that the reactants form an emulsion droplet. The repulsion parameter between inside and outside solvents is set to 100, which is typically used for representing a water-oil system. The emulsion droplet is first equilibrated for 200 000 timesteps before the initiation of polymerization. The *in silico* ATRP copolymerization process involves elemental reactions of initiation, propagation, and crosslinking, which is detailed in Ref. 2. The polymerization produces linear polymer strands with beads linked to each other. Each polymer bead is subject to harmonic bond potential $E_{\text{bond}} = 0.5K_{\text{bond}}\left(r-r_0\right)^2$ and angle potential $E_{\text{angle}} = K_{\text{angle}}\left(1+\cos\theta\right)$. Here, K_{bond} and K_{angle} are the bond and angle strengths, r_0 is the equilibrium bond length, and θ is the angle between two consecutive bonds. To avoid unphysical bond crossing in DPD, we choose a parameter set of $K_{\text{bond}} = 128$, $r_0 = 0.5$ and $K_{\text{angle}} = 4$ according to previous studies.[2,3] The generated microgel is then extracted from the emulsion system and resuspended in a new simulation box filled with aqueous solvent. Another equilibration run is conducted at a specific temperature of interest and the equilibrium microgels are then used in the later SMD simulations. Figures. S1a-d shows the snapshots of the microgels with 5% of crosslinkers in equilibrium at temperatures of 285 K, 308 K, 311 K, and 331 K. A volume phase transition can be clearly observed as the microgel changes from a swollen state to the collapsed state. The microgel features dangling chains at its surface and polymer density decreases from the center to the surface, as shown in Figure S1e. This behavior is consistent with

what observed in real microgels.[4,5] The radii of gyration of the microgels at different temperatures and for different crosslinking densities are plotted in Figures S1f and S1g.

C. Polymer-solvent interactions at different temperatures

In DPD simulations of thermoresponsive microgels, the temperature dependence of the polymer-solvent interaction has been established by relating the bead repulsion $a_{ij}(T)$ to the Flory-Huggins interaction parameter $\chi(T)$. [2,6] Our simulation system (after ATRP) involves two bead types: polymer and water. The repulsion parameters between the same bead type are set to $a_{\mathrm{pp}} = a_{\mathrm{ss}} = a = 25$, with the subscripts represent polymer and water, respectively. The repulsion between the unlike beads, a_{ps}, relates to the Flory-Huggins χ_{ps} parameter given by $a_{\mathrm{ps}} = a + k_{\mathrm{B}}T\chi_{\mathrm{ps}} / 0.306$ [1]. The χ_{ps} parameter for thermoresponsive polymers such as PNIPAM is typically dependent on temperature and polymer concentration of the gel ϕ_{p} [7–9] with a relationship as $\chi_{\mathrm{ps}}(T,\phi) = \chi_1(T) + \chi_2\phi_{\mathrm{p}}$. The first term relates to the respective enthalpy and entropy changes by $\chi_1(T) = (\delta h - T\delta s)/k_{\mathrm{B}}T$. We choose $\delta h = -14.331\times10^{-14}$ erg, $\delta s = -5.425\times10^{-16}$ erg$\cdot$K^{-1}, and $\chi_2 = 0.596$, which is close to the values reported in experiments.[8] This setup in DPD results in a model PNIPAM microgel with a transition temperature about 32 °C.[2]

D. Relationship between simulation and experiment length and time scales

Each water bead in our simulations represents 12 water molecules,[6,10,11] thus one DPD bead has a volume of 360 Å^3. Matching the number density in DPD simulations $\rho_0 = 3\,r_{\mathrm{c}}^{-3}$ and the experimental water density 1 g/cm^3 yields the characteristic length $r_{\mathrm{c}} = 1.03$ nm and the characteristic mass $m = 216$ Da. Since all beads have the same mass in DPD, a coarse-grained

Journal Pre-proofs

polymer bead represents 1.9 N-isopropylacrylamide (NIPAM) monomers. Knowing the characteristic length and energy yields the intrinsic time scale $\tau_{\text{intrinsic}} = \left(m r_c^2 / k_B T_0 \right)^{0.5} = 9.6$ ps. Since DPD has a soft potential that accelerates the dynamics, the characteristic time scale needs to be rescaled to match the physical collective diffusion coefficient of the polymer network, which gives $\tau_{\text{DPD}} = 0.87$ ns[2].

References

(1) Groot, R. D.; Warren, P. B. Dissipative Particle Dynamics: Bridging the Gap between Atomistic and Mesoscopic Simulation. *J. Chem. Phys*. **1997**, *107*, 4423–4435.

(2) Yong, X.; Kuksenok, O.; Matyjaszewski, K.; Balazs, A. C. Harnessing Interfacially-Active Nanorods to Regenerate Severed Polymer Gels. *Nano Lett.* **2013**, *13*, 6269–6274.

(3) Chen, S.; Olson, E.; Jiang, S.; Yong, X. Nanoparticle Assembly Modulated by Polymer Chain Conformation in Composite Materials. *Nanoscale* **2020**, *12*, 14560–14572.

(4) Plamper, F. A.; Richtering, W. Functional Microgels and Microgel Systems. *Acc. Chem. Res.* **2017**, *50*, 131–140.

(5) Stieger, M.; Richtering, W.; Pedersen, J. S.; Lindner, P. Small-Angle Neutron Scattering Study of Structural Changes in Temperature Sensitive Microgel Colloids. *J. Chem. Phys.* **2004**, *120*, 6197–6206.

(6) Hoppe Alvarez, L.; Eisold, S.; Gumerov, R. A.; Strauch, M.; Rudov, A. A.; Lenssen, P.; Merhof, D.; Potemkin, I. I.; Simon, U.; Wöll, D. Deformation of Microgels at Solid–Liquid Interfaces Visualized in Three-Dimension. *Nano Lett.* **2019**, *19*, 8862–8867.

(7) Hirotsu, S. Phase Transition of a Polymer Gel in Pure and Mixed Solvent Media. *J. Phys. Soc. Japan* **1987**, *56*, 233–242.

(8) Hirotsu, S. Softening of Bulk Modulus and Negative Poisson's Ratio near the Volume Phase Transition of Polymer Gels. *J. Chem. Phys.* **1991**, *94*, 3949–3957.

(9) Quesada-Pérez, M.; Maroto-Centeno, J. A.; Forcada, J.; Hidalgo-Alvarez, R. Gel Swelling Theories: The Classical Formalism and Recent Approaches. *Soft Matter* **2011**, *7*, 10536.

(10) Füchslin, R. M.; Fellermann, H.; Eriksson, A.; Ziock, H.-J. Coarse Graining and Scaling in Dissipative Particle Dynamics. *J. Chem. Phys.* **2009**, *130*, 214102.

(11) Spaeth, J. R.; Kevrekidis, I. G.; Panagiotopoulos, A. Z. A Comparison of Implicit- and Explicit-Solvent Simulations of Self-Assembly in Block Copolymer and Solute Systems. *J. Chem. Phys.* **2011**, *134*, 1–13.

Journal Pre-proofs

Supplemental Figures

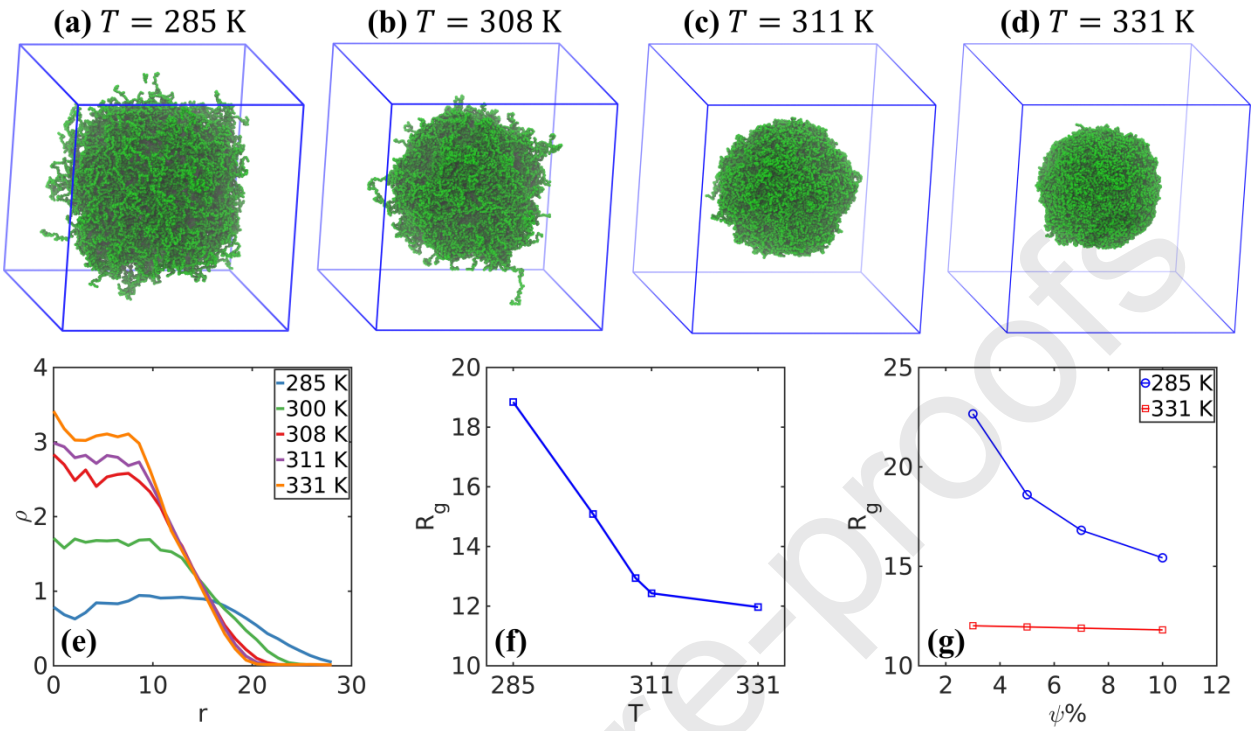

Figure S1. (a)-(d) Snapshots of microgel with 5% crosslinker at equilibrium for temperatures 285 K, 300 K, 311 K, and 331 K, respectively. (e) Corresponding polymer density profiles and (f) radii of gyration of equilibrium microgels with 5% crosslinker at different temperatures. (g) Radii of gyration of microgels with different crosslinker densities in the swollen and collapsed states at low (285 K) and high (331 K) temperatures, respectively.

Journal Pre-proofs

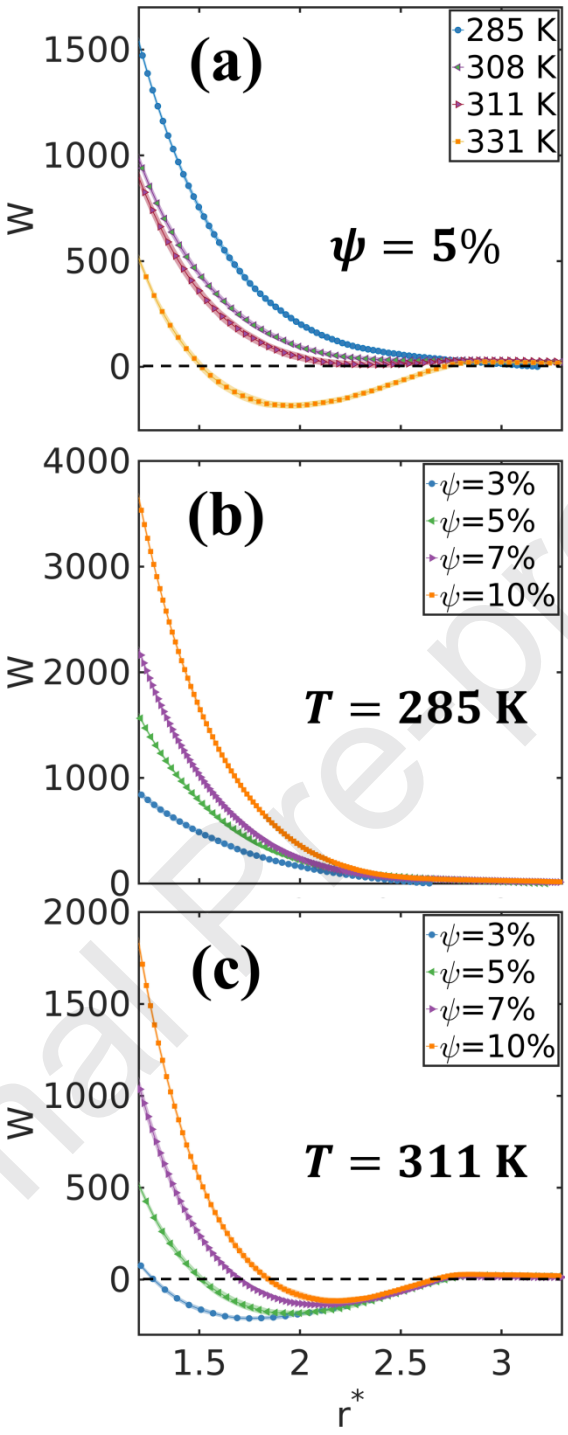

Figure S2. (a) Accumulated work done during SMD simulations for microgels with crosslinker densities of 5% at temperatures 285 K, 308 K, 311 K, and 331. (b, c) Accumulated work profiles for microgels of different crosslinking densities in the swollen (285 K) and collapsed (311 K) states. The error bars represent standard deviation of 10 SMD trajectories.

Journal Pre-proofs

Supplemental Table

Table S1. The fitting exponent n and interaction strength ε in the theoretical model $U(r,T) = \varepsilon(\sigma / r)^n + \Delta f_s(r,T)$ at different temperatures and crosslinking densities.

T, ψ	3%	5%	7%	10%
285 K	n = 3.0, ε = 1300	n = 4.0, ε = 3400	n = 4.2, ε = 3500	n = 5.0, ε = 9500
308 K	n/a	n = 4.1, ε = 2400	n/a	n/a
311 K	n/a	n = 4.2, ε = 2000	n/a	n/a
331 K	n = 3.2, ε = 1250	n = 4.4, ε = 2500	n = 4.4, ε = 3800	n = 5.9, ε = 9000

Journal Pre-proofs

Supplemental Videos

Videos S1-S3: Representative SMD trajectories of microgels with 5% crosslinking density being pulled together at temperatures 285 K, 311 K, and 331 K, respectively. The blue beads represent polymer beads and water beads are not shown for clarity.

Journal Pre-proofs

Shensheng Chen: Conceptualization, Methodology, Software, Investigation, Visualization, Writing - Original Draft; **Xin Yong:** Visualization, Supervision, Writing - Reviewing and Editing.

Journal Pre-proofs

Declaration of interests

☒ The authors declare that they have no known competing financial interests or personal relationships that could have appeared to influence the work reported in this paper.

☐The authors declare the following financial interests/personal relationships which may be considered as potential competing interests:

Journal Pre-proofs